Filament bunch formation upon femtosecond laser pulse propagation through the turbulent atmosphere. Part 1. Method

S.A. Shlenov and V.P. Kandidov

International Educational-Scientific Center at the M.V. Lomonosov Moscow State University, Moscow

Received May 17, 2004

The approach of a steady state case is being suggested and grounded for numerical investigation of the filamentation at propagation of a high-power femtosecond laser pulse in the turbulent atmosphere. This approach is based on the model of phase screens with the spatial spectrum of refractive index fluctuations covering the inertial and dissipative ranges. This approach can be used in analyzing spatiotemporal traces of hot spots in the pulsed laser beam cross section, which cause the formation of a bunch of random filaments, and in studies of the statistical characteristics of this bunch.

The propagation of high-power femtosecond laser pulses in air is accompanied by the phenomenon of filamentation, during which a significant part of the radiation energy is concentrated in hot spots within the beam cross section, observed as extended thin filaments. The first experiments,[1–3] in which long (tens of meters) filaments were observed in air, were conducted with the use of the femtosecond-duration (150–230 fs) pulses of radiation emitted from a Ti:Sapphire laser at the wavelength of 775–800 nm. In these experiments, more than 10% of the initial pulse energy proved to be localized in thin filaments about 100 μm in diameter near the axial area of the beam. In the experiments[4] conducted later on, the filaments were observed at the wavelengths of 795 and 1053 nm at the pulse duration from 60 to 525 fs. In the field experiments conducted in the Observatory of Thuringia (Germany),[5] a pulsed laser beam at the wavelength of 800 nm was observed up to the height of 9 km, and the scattering of laser radiation was detected from aerosol layers at the height of 20 km.

The formation of filaments is initiated due to the Kerr effect, which causes self-focusing of the beam in air. The increase of the intensity at the nonlinear focus is restricted by defocusing in laser plasma formed due to multiphoton and tunnel ionization of oxygen and nitrogen molecules of the air. As a result, the peak intensity in a filament does not exceed 10^{14} W/cm^2 for near-IR pulses with the wavelength of 770–800 nm (Ref. 6). To explain the extended size of the filaments, models of moving focus,[3] self-induced light guides,[2] and "pulsating" focus[7] are being invoked.

The filament is initiated with the highest probability at the beam axis at a distance corresponding to the point of nonlinear focus within the pulsed volume near the power peak. In practice, various causes may lead to the shift of the filamentation point both across and along the direction of the beam propagation. They can be, for example, distortions in the intensity and phase distributions of the beam at the exit from a femtosecond laser system, random angular deviations of the beam, or its incomplete spatial coherence, resulting in irregular shifts of the filament positions from pulse to pulse.[8]

As the pulse propagates through the atmosphere, nucleation of nonlinear focuses is significantly affected by the turbulent fluctuations of the refractive index, leading to the random character of filamentation and wandering of the filaments. Therefore, we can speak about the place of filamentation only in the probabilistic sense. Statistical characteristics of formation of a single filament at the atmospheric path have been studied experimentally and numerically in Refs. 9 and 10. It was established that spatial wandering of a filament obeys the Rayleigh distribution.

With the increasing peak power of the output laser radiation, the filamentation pattern becomes more complicated.[11] In the case that the critical power P_{cr} is exceeded several times, more than one filament are formed in the beam. The process of multifilamentation of a pulse with strong initial distortions of the light field, whose scale corresponded to maximum increment of the modulation instability development in a medium with the Kerr nonlinearity, was considered in Ref. 12. This circumstance caused the formation of filaments in the collimated 200-fs duration pulse with the peak power $P = 35\ P_{cr}$ already at the distance of 8 m from the exit aperture. Mlejnek with co-workers[12] succeeded in observing the dynamics of filamentation in different time layers of the pulse.

During the propagation of high-power femtosecond pulse through the turbulent atmosphere, random fluctuations of the refractive index initiate small-scale self-focusing. Phase fluctuations in the beam transform into the intensity fluctuations and play the role of "nuclei" for the formation of multiple filaments.[13] As a result, a bunch of filaments is formed with the filaments arranged chaotically in the plane of the beam cross section and beginning at different distances from the exit aperture of the laser system. The pattern of filamentation and the properties of the filament bunch depend significantly on the statistical properties

0235-6880/04/08 565-06 $02.00

of the atmospheric turbulence.[14,15] Thus, the process of formation of many filaments in terawatt femtosecond-duration laser pulses is stochastic in principle.

The phenomenon of filamentation is accompanied by the generation of a white-light pulse,[16] which is of interest as a source of radiation for broadband laser sensing of the atmosphere.[5] The stochastic nature of multiple filamentation and, consequently, generation of the sensing pulse can be a cause of instability of lidar returns recorded with femtosecond lidars.[13] In this connection, the study of multiple filamentation of high-power femtosecond laser pulse in the turbulent atmosphere is quite urgent.

This paper develops the technique of computer experiment for studying the initial stage of formation of a filament bunch upon propagation of a high-power femtosecond-duration laser pulse through the turbulent atmosphere. The technique is based on the model of phase screens, encompassing the inertial and dissipative ranges of turbulence, in which the spatial scales of refractive index fluctuations are close to the transverse dimensions of the laser beam and the filament.

Model of beam propagation

In the final formulation, the problem of filamentation of a high-power laser pulse in the atmosphere leads to a multidimensional nonstationary stochastic problem of nonlinear optical interaction of the radiation with a medium, and its solution requires huge computational resources. However, the initial stage of filamentation in a laser pulse is mostly determined by the Kerr nonlinearity and turbulent fluctuations of the atmospheric refractive index $\tilde{n}(x,y,z)$. The initial stage of filamentation is understood here as the nonlinear increase of intensity in the beam or its fragments until the generation of laser plasma. Further in the filamentation process, a complex spatiotemporal dynamics of the light wave field appears, which reflects the competitive processes of radiation concentration in nonlinear focuses on the one hand and the diffraction divergence, dispersion spreading, and defocusing due to generation of plasma on the other hand.

Because the generation of filaments and their spatial positions are determined by the small-scale self-focusing, which develops before the break of the pulse into short sub-pulses, the material dispersion can be neglected in numerical simulation of the filament bunch formation. In addition, we can neglect the contribution of plasma nonlinearity, because multiphoton ionization, leading to the generation of the laser-induced plasma, occurs at the light field intensity on the order of 10^{14} W/cm^2, which is achieved only after the energy concentration at the nonlinear focus.

The assumptions accepted allow us to reduce the study of multifilamentation of a laser pulse in the turbulent atmosphere to the three-dimensional stationary stochastic problem of small-scale self-focusing, in which time plays the role of a parameter. Within the framework of the method of slowly varying amplitudes, this problem is known,[17] to have singularities at the nonlinear focus, which prevents considering the pulse propagation at the distance exceeding the length of formation of the first nonlinear focus. At the same time, in the model of multifilamentation it is important to have the possibility of analyzing the successive formation of filaments. Toward this end, the simple model of Kerr nonlinearity with saturation is used, in which the radiation intensity at the already formed nonlinear focuses in the beam cross section is restricted to the level $I \sim 10^2 I_0$ (I_0 is the peak intensity at the output from the laser system).

Thus, the initial stage of filamentation upon the propagation of the femtosecond pulse can be described by the following equation for the slowly varying amplitude $E(x,y,z,t)$ of the light field:

$$2ik_0\left(\frac{\partial E}{\partial z}+\frac{1}{V_g}\frac{\partial E}{\partial t}\right)=\Delta_\perp E+\frac{2k_0^2}{n_0}\Delta n_{nl}(I)E+$$

$$+\frac{2k_0^2}{n_0}\tilde{n}(x,y,z)E, \qquad (1)$$

where k_0 is the wave number; $\Delta n_{nl}(I)=n_2 I_s \arctan(I/I_s)$ is the nonlinear addition to the refractive index, which saturates with the increasing intensity I, and the parameter I_s is the intensity of saturation at the nonlinear focus; V_g is the group velocity. This formulation of the problem allows us to reconstruct the appearance of a next filament in the beam cross section under conditions of developed filamentation. The coefficient n_2 for the pulses shorter than 100 fs includes the contributions of the practically instantaneous response of the electron polarizability and the inertial response, which is determined by the stimulated Raman scattering at rotational transitions of air molecules and depends on the pulse shape,[7,8,18] to the cubic nonlinearity. The fluctuations of $\tilde{n}(x,y,z)$ are responsible for the random character of filamentation through disturbing the light field in the pulse cross section.

The complex amplitude of the light field $E(x,y,z=0,t)$ at the exit aperture of the laser system is set in the form of the Gaussian dependences on the spatial coordinates x, y and the time t:

$$E(x,y,z=0,t)=E_0\exp\left\{-\frac{x^2+y^2}{2a_0^2}\right\}\exp\left\{-\frac{t^2}{2\tau_0^2}\right\}, \qquad (2)$$

where a_0 is the beam radius; τ_0 is the pulse duration. During the femtosecond pulse, the turbulence can be believed frozen, and, consequently, the time t in Eq. (1) is the parameter determining the power of a time layer of the pulse.

Thus, for the known field of fluctuations of the refractive index of the medium $\tilde{n}(x,y,z)$, the system of equations (1), (2) allows the calculation to be made of the stochastic light field at the distance z from the exit aperture of the femtosecond laser system. As a hot spot with the intensity exceeding some threshold

value I_p appears in the beam, formation of the next filament is observed. The spatial coordinates x, y, z of the hot spot determine the position of the filament in the cross section plane XOY at the distance z and at the threshold value $I_p \geq 75\, I_0$ quite accurately, because the intensity increases explosively in approaching the nonlinear focus, tending to infinity within the method of slowly varying amplitudes.

The nonlinear-optical transformation of the laser pulse during filamentation significantly enriches the spatial spectrum of the light field, expanding the range of scales of its variability in the plane perpendicular to the direction of propagation.[19] To determine the lower boundary of these scales, let us estimate the characteristic size of these perturbations, which are centers of filamentation.

In a medium with the cubic nonlinearity, instable perturbations are those, whose cross sections contain the power exceeding the critical power of self-focusing.[20] In air the critical power of self-focusing for radiation at the wavelength $\lambda = 800$ nm is $P_{cr} = 6 \cdot 10^9$ W (Ref. 3). As the pulse shortens to 20–50 fs, the effective value of P_{cr} increases up to $12 \cdot 10^9$ W because of the inertia of the nonlinear response connected with the stimulated scattering at rotational transitions of the nitrogen molecule.[7,8,18] In pulses, which are usually used in modern filamentation experiments, the peak intensity is $I_0 = 10^{10}$–10^{11} W/cm^2 (Refs. 1–6). The smallest size of perturbations r_{cr} in the profile of the beam, which contains the power exceeding the power of self-focusing, can be estimated from the condition $\pi r_{cr}^2 I_0 \geq P_{cr}$. Hence we obtain $r_{cr} \geq 0.1$–0.5 cm. At the beam periphery, where the intensity is lower, r_{cr} increases. At filamentation of the pulse, the scale of spatial localization of the light field can be taken equal to the filament radius r_{fil}, which is $r_{fil} \approx 5 \cdot 10^{-2}$ cm according to the experimental data.[1–3] Thus, in the process of filamentation, the characteristic size of spatial inhomogeneities of the light field in the cross section plane can decrease ten and more times.

At the surface atmospheric paths, the scale of fluctuations of the refractive index of the air varies, according to the model of developed turbulence, from the inner scale $l_0 = 1$–0.1 cm to the outer scale L_0, which can amount to tens of meters.[21] The comparison of the scales of spatial inhomogeneities of the atmosphere and pulse suggests that if all significant perturbations of the light field initially fall within the inertial range of atmospheric turbulence, then in the process of filamentation a significant part of perturbations shifts into the dissipative range of turbulence. Thus, the atmospheric inhomogeneities of the same scale $l \geq r_{cr}$ are small-scale for the pulse at the stage of formation of filaments and large-scale for already formed filaments, because the areas of random focusing, containing the critical power, lie in the inertial range of atmospheric turbulence, while the inhomogeneities of the light field associated with a filament lie in the dissipative range. In numerical simulation of the stochastic problem of filamentation upon the propagation of high-power femtosecond laser pulses, it is of great significance the imitation of fluctuations of the refractive index in the dissipative range of atmospheric turbulence.

Inhomogeneities of the refractive index $\tilde{n}(x,y,z)$, close in size to the outer scale L_0, determine the global tilt of the beam wave front and, consequently, the angular shift of the whole set of the filaments formed. Thus, the numerical study of the process of filamentation upon the propagation of high-power femtosecond laser pulses along open atmospheric paths requires adequate reconstruction of the refractive index fluctuations in a wide range of spatial scales, covering both the inertial and the dissipative ranges. This determined the choice of the most complete model of atmospheric turbulence.

Model of phase screens

In this work, we use the classical model of atmospheric turbulence with the modified Karman spectrum of spatial fluctuations of the refractive index[21]:

$$F_n(\kappa_x, \kappa_y, \kappa_z) = 0.033 C_n^2 \left(\kappa^2 + \kappa_0^2\right)^{-11/6} \exp\left(-\kappa^2 / \kappa_m^2\right), \quad (3)$$

which covers both the inertial and the dissipative ranges. Here, the structure constant C_n^2 characterizes the value of turbulent fluctuations, while the constants $\kappa_0 = 2\pi/L_0$ and $\kappa_m = 5.92/l_0$ characterize the lower and upper boundaries of the spatial frequencies of the inertial range.

Fluctuations of $\tilde{n}$ are taken into account within the framework of the model of phase screens on the assumption that the random effect of a layer of the turbulent medium on the light beam manifests itself at the distances Δz longer than the outer scale of turbulence L_0 and the length of diffraction conversion of the phase perturbations of the light field into the amplitude ones. In simulating the turbulent fluctuations of $\tilde{n}$, this allows us to "shrink" the turbulent medium layer of the finite thickness Δz into a thin phase screen and believe that these screens are δ-correlated along the direction z of the beam propagation. The allowance for the longitudinal correlation of turbulent fluctuations of the refractive index in the model of phase screens is considered thoroughly in Ref. 22. The spectral density of the phase fluctuations on the δ-correlated screen has the form

$$F_\varphi(\kappa_x, \kappa_y) = 2\pi k_0^2 \Delta z F_n(\kappa_x, \kappa_y, 0). \quad (4)$$

The spectral method was successfully used[23] to reconstruct the random field of spatial phase fluctuations $\tilde{\varphi}(x,y)$. This method is based on summation of the Fourier harmonics of the spatial spectrum, whose amplitudes are δ-correlated random numbers with the weighting factors a_{pq}. The values of these factors are selected to obtain the given mean spectral density of phase fluctuations on the screen (4). In practice, it is convenient to generate complex fields, in which the real and imaginary parts can be considered as two independent phase screens.

According to the spectral method, the random realization of the complex two-dimensional field of phase fluctuations φ_{nm} at the nodes of a uniform computational grid n, m is determined by the equation

$$\varphi_{nm} = \frac{1}{\sqrt{NM}} \sum_{p=-N/2}^{N/2-1} \sum_{q=-M/2}^{M/2-1} a_{pq}(\xi_{pq} + i\eta_{pq}) W_N^{pn} W_M^{qm}, \quad (5)$$

where N and M are the numbers of nodes of the computational grid along the transverse coordinates, x and y; the statistically independent random numbers ξ_{pq}, η_{pq} are distributed uniformly over the range $\left[-\sqrt{3},\sqrt{3}\right]$; $W_N = \exp\left\{i\frac{2\pi}{N}\right\}$. The weighting factor a_{pq} depend on the spectral density of phase fluctuations (4) as follows:

$$a_{pq}^2 = F_\varphi(p\Delta\kappa_x, q\Delta\kappa_y)\Delta\kappa_x\Delta\kappa_y . \quad (6)$$

The steps of the computational grid in the spectral space $\Delta\kappa_x$, $\Delta\kappa_y$ are connected with the transverse dimensions of the phase screen L_x and L_y as

$$\Delta\kappa_x = 2\pi/L_x, \ \Delta\kappa_y = 2\pi/L_y. \quad (7)$$

Note that in the random field formed by the spectral method, false correlation arises at the scale $r > L_x/2$, $L_y/2$, due to the spatial periodicity of the summed Fourier harmonics. Therefore, strictly speaking, only a quarter of the obtained screen should be used in problems with the model random fields (5).

The spectral method (5) is efficient for generation of random fields, because it allows the use of the Fast Fourier Transform (FFT) algorithm in computations. However, the maximum size of phase inhomogeneities on the screen is inversely proportional to the step of spatial frequencies $\Delta\kappa_x$, $\Delta\kappa_y$ and, according to Eq. (7), it is restricted by the dimensions L_x, L_y of the screen. This circumstance prevents from taking into account, within the standard spectral approach, the effect of large-scale inhomogeneities of the refractive index on the beam phase without simultaneous increasing the screen size in the range of scales far larger than the beam aperture with the following separation of the small part of the screen. The latter circumstance implies a significant increase in the computational resources used and thus drastically decreases the attraction of the spectral method for numerical simulation of random fields with a wide spectrum of spatial fluctuations. Various modifications of the spectral method based on the use of additional information about the low-frequency wing of the spectrum were proposed to solve this problem.[24]

A method based on superposition of two separate phase screens is described in detail in Ref. 25. One screen containing the high and middle spatial frequencies of phase fluctuations is formed by the spectral method, while the other one, reconstructing the low frequencies, is formed by superposition of Zernike or Karhunen–Loeve polynomials.

In this work, we use the modified spectral method.[24] According to this method, the consecutive (iterative) concentration of nodes of the computational grid is performed in the spectral space κ_x, κ_y in the vicinity of zeroth harmonics (Fig. 1).

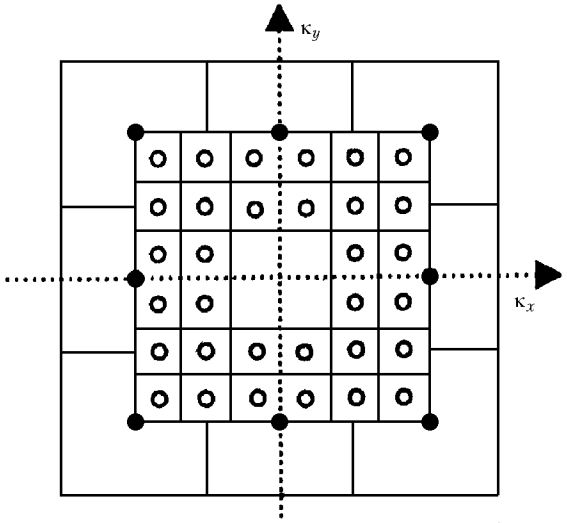

Fig. 1. Concentration of the computational grid in the spectral space in simulating random phase screens by the modified spectral method[24]; nodes of the standard grid (closed circles), first iteration of the concentrated nodes of the low-frequency grid with subharmonics (open circles).

At the first iteration, additional 32 harmonics are calculated with the step $\Delta\kappa_x/3$ and $\Delta\kappa_y/3$ in the rectangular region of the spectral space bounded by the points with the coordinates $(-\Delta\kappa_x, \Delta\kappa_y)$, $(\Delta\kappa_x, -\Delta\kappa_y)$ (Fig. 1). The low-frequency harmonics obtained in this way are called subharmonics. The next, second iteration, is performed through similar condensation of nodes in the low-frequency spectral region with the coordinates $(-\Delta\kappa_x/3, \Delta\kappa_y/3)$, $(\Delta\kappa_x/3, -\Delta\kappa_y/3)$, and so on.

The contribution of the low-frequency spectral component to the resulting phase screen is described by the equation

$$\varphi_{nm}^{\mathrm{LF}} = \sum_{k=1}^{N_k} 3^{-k} \frac{1}{\sqrt{NM}} \times$$

$$\times \sum_{p=-3}^{2} \sum_{q=-3}^{2} a_{pq}\left(\xi_{pq} + i\eta_{pq}\right) W_N^{3^{-k}(p+0.5)n} W_M^{3^{-k}(q+0.5)m}, \quad (8)$$

where

$$a_{pq}^2 = F_\varphi\left[3^{-k}(p+0.5)\Delta\kappa_x, 3^{-k}(q+0.5)\Delta\kappa_y\right]\Delta\kappa_x\Delta\kappa_y,$$

$k = 1, \ldots, N_k$ is the number of the iteration.

The grid function $\varphi_{nm}^{\mathrm{LF}}$ is calculated through direct summation of the expression (8) without the use of fast algorithms, and therefore it is important to restrict the number of iterations N_k. In practice, four iterations are usually sufficient for construction of phase screens with the correlation functions satisfactorily describing atmospheric fluctuations.[26]

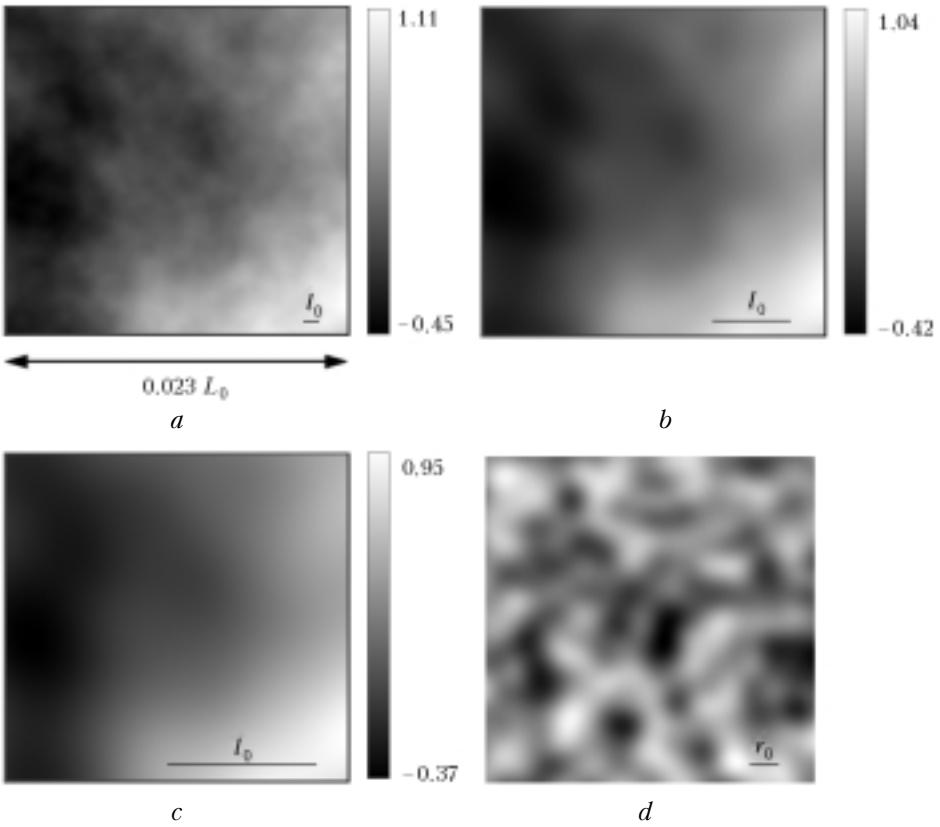

Fig. 2. Phase screens with the spectrum (4) and (3), imitating the refractive index fluctuations at the length Δz = 10 m with the structure constant $C_n^2 = 1.5 \cdot 10^{-14}$ cm$^{-2/3}$, the outer scale L_0 = 1 m, and the inner scale l_0 = 1 (*a*), 5 (*b*), and 10 mm (*c*). Screen fragments with the dimensions 2.3 × 2.3 cm ($L_x = L_y$ = 9.2 cm) are shown. For a comparison, the right bottom panel shows the screen with the Gaussian spectral density and the correlation length r_0 = 1.8 mm (*d*).

As an illustration, Fig. 2 shows some realizations of phase screens synthesized by the modified spectral method with $N_k = 4$. The value of the phase fluctuations on the screen is shown by the grades of gray. The outer scale of turbulence L_0 more than 10 times exceeds the dimensions L_x and L_y. In the realizations, one can clearly see the global tilt of the phase front from the left top to the right bottom. Along with the global variation of the phase due to large-scale fluctuations with the size on the order of L_0, there are smaller phase fluctuations looking like dark and light spots of irregular shapes.

The effect of the inner scale l_0 of atmospheric turbulence with the spectrum (3) on the phase fluctuations is demonstrated by the series of the screens shown in Figs. 2*a*, *b*, and *c*, which are synthesized with the same set of random amplitudes ξ_{pq} and η_{pq} of the spectral components, but with different values of the inner scale l_0. The parameter l_0 varies from 1 to 10 mm as going from Fig. 2*a* to Fig. 2*c*. The value of l_0 is illustrated by the bars at the lower right of each figure. Since the smallest size of phase fluctuations is restricted by the inner scale of turbulence l_0, we can see the smoothing of small-scale phase fluctuations with the increase of l_0.

For a comparison, Fig. 2*d* depicts the phase screen drawn for the Gaussian spectrum of fluctuations. One can see that this screen, including inhomogeneities of only one scale, is too a rough model of the atmospheric turbulence and cannot be used in stochastic simulation of the phenomenon of filamentation.

The structure function of phase fluctuations $D_\varphi(\rho)$ [Ref. 21] obtained by averaging over 100 realizations of statistically independent screens is shown in Fig. 3 as a solid curve for small values of the argument ρ. The dashed curve shows the same function for the screens constructed by the spectral method for the same parameters of turbulence and the computational grid, but without using the algorithm of addition of subharmonics (8). The comparative analysis of these two functions shows that, without using subharmonics, the effect of saturation of the structure function of phase fluctuations, connected with periodicity of random fields in the spectral method, begins to manifest itself rather quickly. Although this effect shows itself in full measure at the scales comparable with the screen dimensions L_x and L_y, the error of the method can exceed 50% even at the diameter of the beam cross section. In Fig. 3, the beam diameter $2a_0 = 1.8$ cm, which is usually used in experiments (see, for example, Refs. 5 and 8) is shown by the vertical bar. The iterative algorithm of addition of subharmonics (8) can significantly improve the quality of generated random phase fields and make their structure function closer to the calculated one.

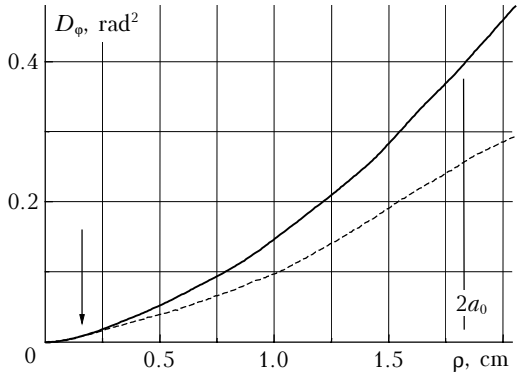

Fig. 3. Structure function of phase fluctuations on the screen $D_\varphi(\rho)$; $C_n^2 = 1.5 \cdot 10^{-14}$ cm$^{-2/3}$, $L_0 = 1$ m, $l_0 = 1$ mm, $\Delta z = 10$ m; averaging done over 100 realizations of the screens drawn by the spectral method with (solid curve) and without (dashed curve) subharmonics. The vertical bar at the right corresponds to the diameter of the laser beam $2a_0$, the left arrow shows the radius of the circular area containing the critical power of self-focusing at the beam power $P_0 = 2 \cdot 10^{11}$ W.

Thus, the stationary approach for studying stochastic multifilamentation of high-power femtosecond laser pulses in the turbulent atmosphere has been proposed and argued; this approach is based on the model of phase screens with the spectrum of spatial refractive index fluctuations covering the inertial and dissipative ranges of the turbulent fluctuations.

Acknowledgments

This work was supported, in part, by the Russian Foundation for Basic Research (grant No. 03–02–16939), the European Office of the US Army Research (contract No. 62558–03–M0029), and CRDF GAP (grant No. RPO–1390–TO–03).

References

1. A. Braun, G. Korn, X. Liu, D. Du, J. Squier, and G. Mourou, Opt. Lett. **20**, No. 1, 73–75 (1995).
2. E.T.J. Nibbering, P.F. Curley, G. Grillon, B.S. Prade, M.A. Franco, F. Salin, and A. Mysyrovicz, Opt. Lett. **21**, No. 1, 62–64 (1996).
3. A. Brodeur, C.Y. Chien, F.A. Ilkov, S.L. Chin, O.G. Kosareva, and V.P. Kandidov, Opt. Lett. **22**, No. 5, 304–306 (1997).
4. B. La Fountaine, F. Vidal, Z. Jiang, C.Y. Chien, D. Corutois, A. Desparois, T.W. Johnston, J.-C. Kieffer, H. Pepin, and H.P. Mercure, Phys. Plasm. **6**, No. 3, 1815–1821 (1999).
5. J. Kasparian, M. Rodriguez, G. Mejean, J. Yu, E. Salmon, H. Wille, R. Bourayou, S. Frey, Y.-B. Andre, A. Mysyrowicz, R. Sauerbrey, J.-P. Wolf, and L. Woste, Science **301**, No. 5629, 61–64 (2003).
6. J. Kasparian, R. Sauerbrey, and S.L. Chin, Appl. Phys. B **71**, 877–879 (2000).
7. M. Mlejnek, E.M. Wright, and J.V. Moloney, Opt. Lett. **23**, No. 5, 382–384 (1998).
8. K.Yu. Andrianov, V.P. Kandidov, O.G. Kosareva, S.L. Chin, A. Talebpour, S. Petit, W. Liu, A. Iwasaki, and M.-C. Nadeau, Izv. Ros. Akad. Nauk, Ser. Fiz. **66**, No. 8, 1091–1102 (2002).
9. S.L. Chin, A. Talebpour, J. Yang, S. Petit, V.P. Kandidov, O.G. Kosareva, and M.P. Tamarov, Appl. Phys. B **74**, 67–76 (2002).
10. V.P. Kandidov, O.G. Kosareva, M.P. Tamarov, A. Brodeur, and S.L. Chin, Quantum Electron. **29**, No. 1, 911–915 (1999).
11. S.L. Chin, S. Petit, F. Borne, and K. Miyazaki, Jap. J. Appl. Phys. Part 2 **38**, No. 2A, L126–L128 (1999).
12. M. Mlejnek, M. Kolesik, J.V. Moloney, and E.M. Wright, Phys. Rev. Lett. **83**, No. 15, 2938–2941 (1999).
13. W. Liu, S.A. Hosseini, B. Ferland, S.L. Chin, O.G. Kosareva, N.A. Panov, and V.P. Kandidov, New J. Phys. **6**, No. 6, 1–22 (2004).
14. S.A. Shlenov, V.P. Kandidov, and O.G. Kosareva, in: *Abstracts of IQEC/LAT-2002,* Moscow (2002), Techn. Dig. (2002), p. 53.
15. S.A. Shlenov, V.P. Kandidov, and O.G. Kosareva, in: *Abstracts of XIth Conf. on Laser Optics (LO'2003),* St. Petersburg (2003), p. 43.
16. V.P. Kandidov, O.G. Kosareva, I.S. Golubtsov, W. Liu, A. Becker, N. Akozbek, C.M. Bowden, and S.L. Chin, Appl. Phys. B **77**, 149–165 (2003).
17. S.A. Akhmanov, A.P. Sukhorukov, and R.V. Khokhlov, Usp. Fiz. Nauk **93**, No. 1, 19–70 (1967).
18. P.A. Oleinikov and V.T. Platonenko, Laser Phys. **3**, No. 3, 618–622 (1993).
19. V.P. Kandidov, Usp. Fiz. Nauk **166**, No. 12, 1309–1338 (1996).
20. V.I. Bespalov, A.G. Litvak, and V.I. Talanov, in: *Nonlinear Optics* (Nauka, Novosibirsk, 1968), pp. 428–463.
21. V.E. Zuev, V.A. Banakh, and V.V. Pokasov, *Optics of the Turbulent Atmosphere* (Gidrometeoizdat, Leningrad, 1988), 270 pp.
22. S.S. Chesnokov, V.P. Kandidov, S.A. Shlenov, and M.P. Tamarov, Proc. SPIE **3432**, 14–25 (1998).
23. L.I. Mirkin, M.A. Rabinovich, and L.P. Yaroslavskii, Zh. Vychisl. Mat. Mat. Fiz. **12**, No. 5, 1353–1357 (1972).
24. E.M. Johansson and D.T. Gavel, Proc. SPIE **2200**, 372–383 (1994).
25. V.P. Lukin and B.V. Fortes, *Adaptive Beaming and Imaging in the Turbulent Atmosphere* (SPIE Press, 2002).
26. V.P. Kandidov, M.P. Tamarov, and S.A. Shlenov, Atmos. Oceanic Opt. **11**, No. 1, 23–29 (1998).